A design of a miniature ultrasonic pump using a bending disk transducer

**Takeshi Hasegawa · Daisuke Koyama ·
Kentaro Nakamura · Sadayuki Ueha**

Abstract If a pipe end is faced at a piston-vibrating surface with a small gap in liquid, the liquid is suctioned into the pipe. The present ultrasonic pump is based on this phenomenon to induce flow. For a low-profile configuration, we introduce a 30-mm-diameter bending disk driven by a ring-shaped PZT element bonded on the back of the disk. The disk vibrator is softly supported by frames via O-rings at its circumference, and is worked at the fundamental resonance frequency of 19 kHz of the bending mode. A pipe is installed perpendicularly to the center of the disk vibrator with a small gap. To improve the pump performance, we seek for the optimum vibration distribution of the disk vibrator. When the thickness around the disk center becomes large, the shape of the vibration distribution near the center approaches to a piston vibrator. If the flatness of the vibration distribution is defined as the vibration amplitude just under the pipe edge divided by the vibration amplitude at the disk center, it is 92.0% for the original bending disk. The flatness of the new design became 98.1% as a result of the optimization of the thickness profile of the disk. The pump pressure became high as the flatness became large when the gap size was small enough. The maximum pump pressure of 20.6 kPa was achieved when the vibration velocity at the disk center was 1.0 m/s and the gap size was 10 μm, while the maximum flow rate of 22.5 ml/min. was obtained with the input electrical power of 3.8 W.

1 Introduction

In these years, miniature fluidic pumps have great demand in the area of water-cooling of central processing unit for desktop personal computers and laptops [1], liquid dispensing system [2–4], fuel delivery system for miniature fuel cells [5, 6], assistant artificial heart pump [7, 8] and medical apparatus [9, 10]. Conventional electromagnetic pump has difficulties in miniaturization in size and suppression of electromagnetic noise. For this reason, several miniature pumps using piezoelectrically [11, 12] or electrostatically [13–15] excited membrane vibration have been proposed. Most of these pumps require valves to control the direction of flow. However, the valves have the problems of wear and clogging due to bubbles and particles. The vibration frequency is low in usual design within the audible range, and noise and vibration will be a difficulty for practical installation. On the other hand, the valve can be eliminated if the acoustic effects of high frequency ultrasound acting directly on fluid such as acoustic radiation force [16] and acoustic streaming [17–20] are used. However, the performance of the pumps using the acoustic effect is low compared with the pumps with valves.

The authors have been investigating the phenomenon of an ultrasonically vibrating surface facing with a pipe via a small gap in water [21, 22]. If the gap is small enough, water is suctioned into the pipe efficiently. The present ultrasonic pump is based on this phenomenon to induce flow. In our primary experiments of the pump, a bolt-clamped Langevin transducer 50 mm in diameter was used.

T. Hasegawa (✉) · D. Koyama · K. Nakamura · S. Ueha
Precision and Intelligence Laboratory,
Tokyo Institute of Technology,
4259-R2-26, Nagatsutacho, Midoki-ku,
Yokohama 226-8503, Japan
e-mail: hasegawa.t.ac@m.titech.ac.jp

This configuration is large in size and power consumption and is not appropriate for required applications.

In this paper, we describe a low-profile configuration with a 30-mm-diameter bending disk transducer. To improve the pump performance, we investigated the optimum vibration distribution of the disk vibrator. When the thickness at the disk center became large, the shape of the vibration distribution around the center approached to a piston vibrator. If the flatness is defined as the vibration amplitude just under the pipe edge divided by the vibration amplitude at the center, it is 92.0% for the original bending disk transducer. The flatness of the new design became 98.1% by optimization the design of the bending disk transducer through finite element method (FEM). The pump pressure became large as the flatness became large when the gap size was small enough. The maximum pump pressure of 20.6 kPa was achieved when the vibration velocity at the disk center was 1.0 m/s and the gap size was 10 μm, while the maximum flow rate of 22.5 ml/min. was obtained with the input power of 3.8 W.

2 Configurations of the miniature ultrasonic pump

Figure 1 shows the miniature configuration using a bending disk transducer. A ring-shaped PZT element (30 mm in outer diameter, 15 mm in inner diameter and 2.0 mm in thickness) is bonded on the back of an aluminum disk (30 mm in diameter and 1.2 mm in thickness). The disk transducer is softly supported by frames and O-rings at its
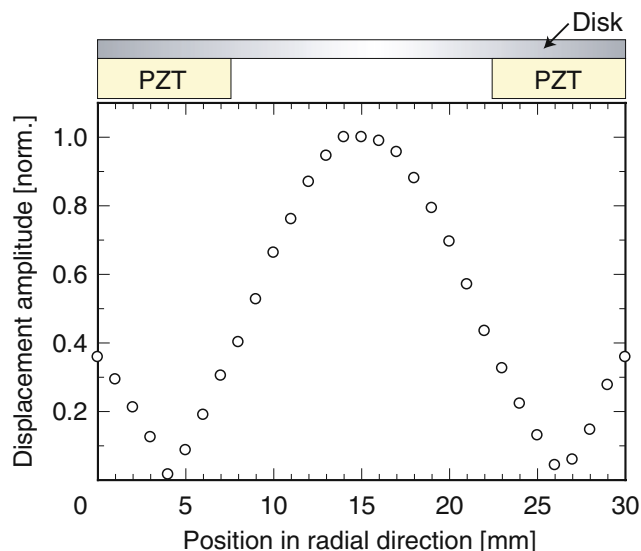

Fig. 2 Vibration distributions in the radial direction of the bending disk transducer

circumference, and is worked at the resonance frequency of 19 kHz of the fundamental bending mode. The measured vibration distribution in the radial direction is shown in Fig. 2. A glass pipe is installed perpendicularly to the disk center with a small gap. The pipe dimensions are 5.0 mm in outer diameter and 3.5 mm in inner diameter. The distance from the vibrating surface to the water surface is 2 mm. The pump performance is evaluated by the pump pressure P and the flow rate Q. P is defined as $\rho g h$ with water density ρ, gravitational acceleration g and water height in the pipe h. Q is defined as the water volume by the pumping per a
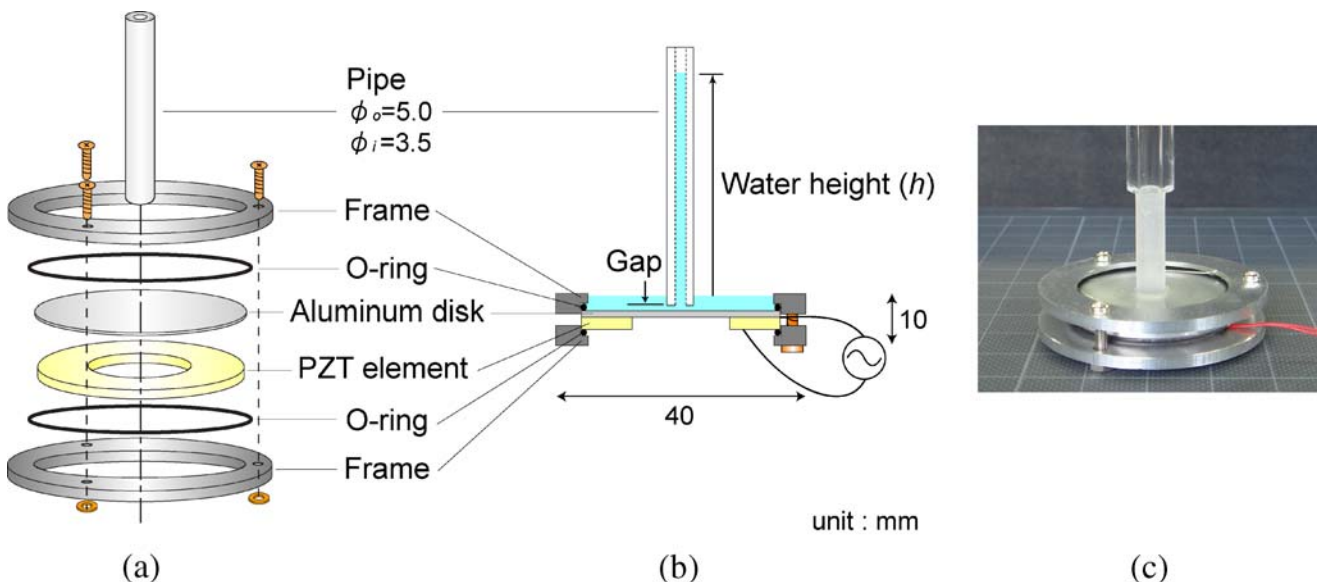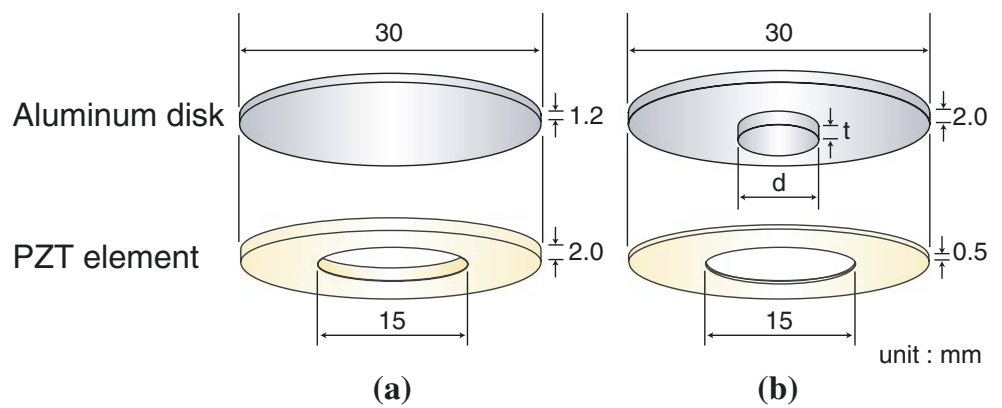

Fig. 1 Configurations of the miniature ultrasonic pump using a bending disk transducer: (a), structure; (b), cross-section; (c), photograph of the prototype pump

minute. The vibration velocity at the disk center is measured by a laser Doppler vibrometer (Polytec CLV-1000).

3 Optimization of the bending disk transducer

To improve the pump performance, we explored the optimum vibration distribution of the bending disk transducer. In our previous study [23], we found that the pump pressure becomes large when the shape of the vibration distribution near the center of the disk approaches to a piston vibrator. Therefore, we propose the new configuration with stepped-convex thickness profile at the disk center in order to obtain an uniform distribution near the center. Figure 3 shows the original and new configurations of the

bending disk transducers, which have the same diameter. To the lower input electrical voltage, the thickness of the PZT element is reduced to 0.5 mm. The results of the experiment showed that the input electrical voltage of 332 V_{pp} is required for the original design to generate the vibration velocity of 1.0 m/s at the disk center, but only 198 V_{pp} for the new design.

First, we investigated the flattening design of the vibration distribution of the bending disk transducer through FEM (ANSYS 9.0) by changing the diameter and thickness of the stepped-convex. Here, we define the flatness of the vibration distribution as the vibration amplitude of the disk under the pipe edge divided by the vibration amplitude of the disk under the pipe center, as shown in Fig. 4. Figure 5 illustrates the calculated results for the flatness of the vibration distribution as functions of the diameter and thickness of the stepped-convex. In the case of 1 mm in thickness of the stepped-convex, the flatness reaches the maximum when the diameter of the stepped-convex is 7 mm. In the same way, the flatness reaches the maximum when the combinations of the diameter and thickness of the stepped-convex:(d,t) are (8,2), (9,3) and
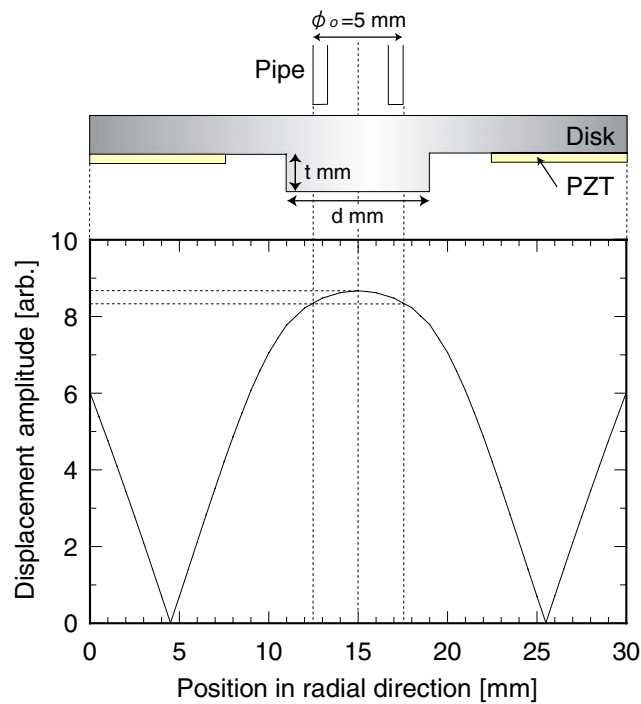

Fig. 4 Definition of the flatness of the vibration distribution
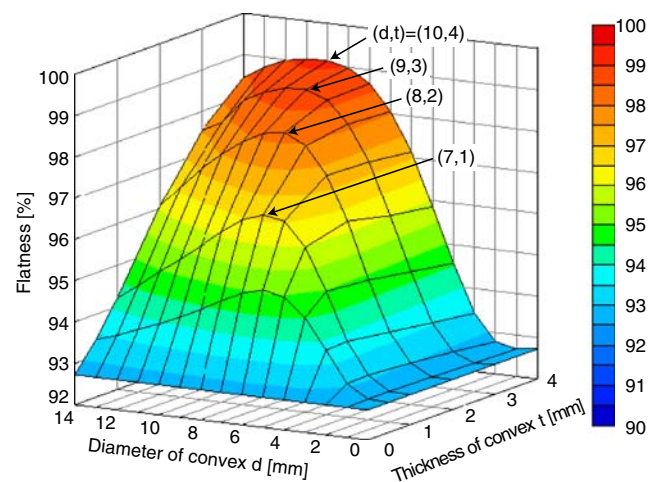

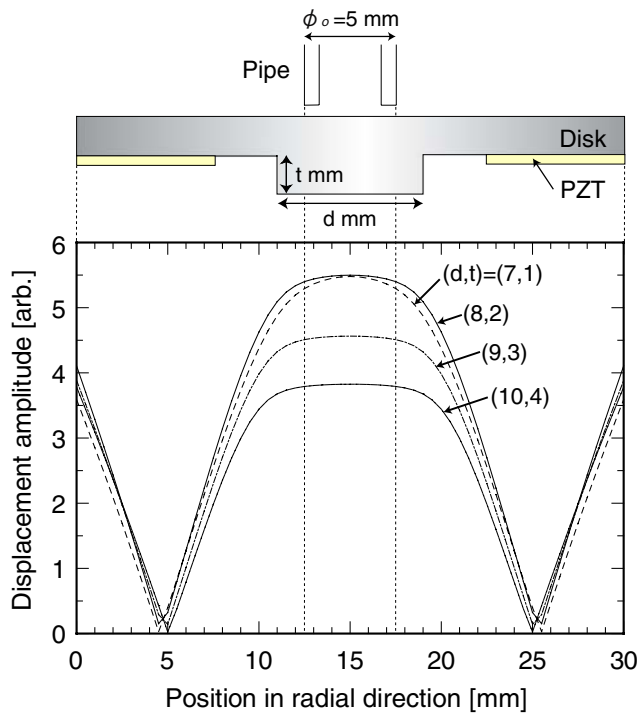Fig. 5 Flatness vs. the diameter and thickness of the stepped-convex

Fig. 6 Vibration distributions in the radial direction using the optimum combination of (d,t)

Fig. 8 Comparison of the vibration distributions of the original with new design

(10,4), respectively. Then, we calculated the vibration distributions for these optimum combinations of (d,t) as shown in Fig. 6. The displacement amplitude at the disk center reaches the maximum when the combination of (d,t) is (8,2). Figure 7 illustrates the displacement amplitude at disk center and the resonance frequency of the disk transducer as functions of the thickness of the stepped-convex. When the thickness of the stepped-convex is larger

than 2.8 mm, the resonance frequency is lower than the human's audible limit (20 kHz). Therefore, the thickness of the stepped-convex is chosen to be 2 mm, among the three combinations mentioned above, $d=8$ and $t=2$ are adopted. Fundamental resonance frequency of the bending disk transducer, quality factor and free motional admittance were 20.1 kHz, 25.2 and 0.6 mS, respectively. Figure 8 shows the radial vibration distributions of the previous and new design. The flatness of the vibration distribution became 92.0% for the previous design, and 98.1% for the new design. The result has shown that the flatness of the vibration distribution increased by about 6% in the new design.
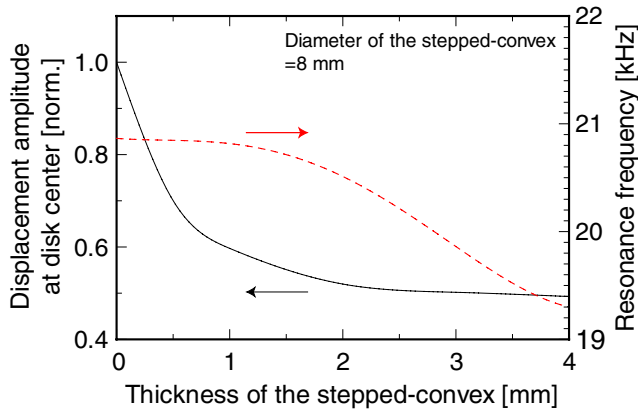

Fig. 7 Displacement amplitude at the center and the resonance frequency of the disk transducer as functions of the thickness of the stepped-convex
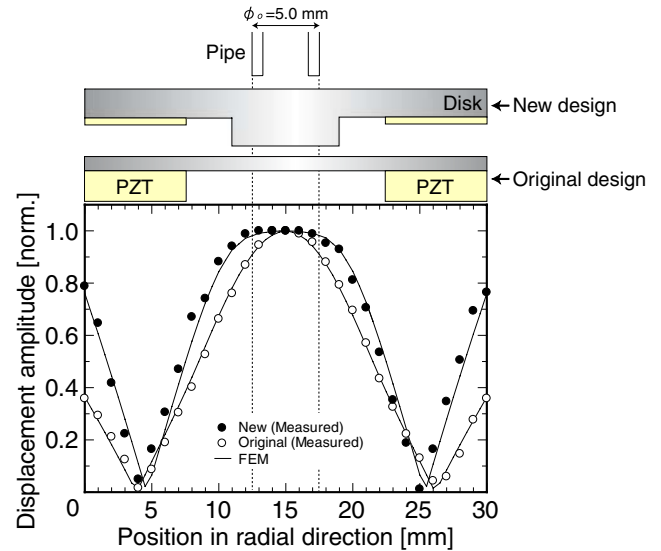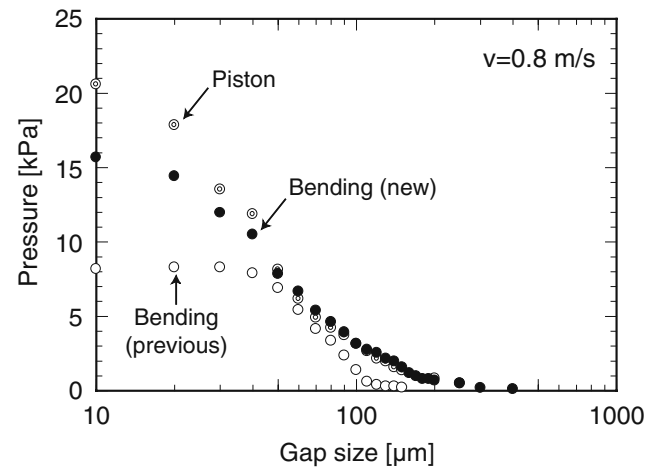

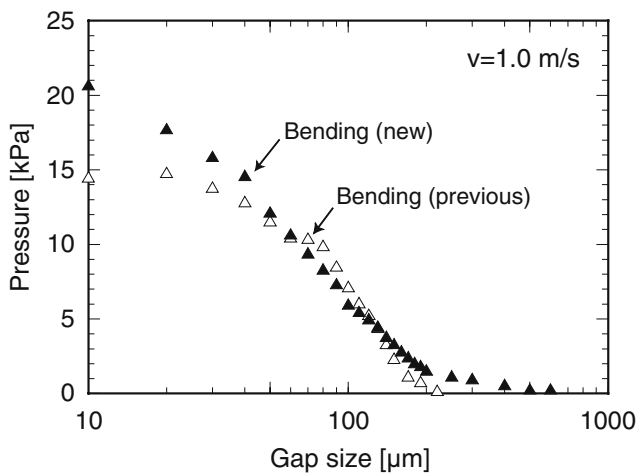Fig. 9 Pump pressure vs. the gap size when the vibration velocity is 0.8 m/s

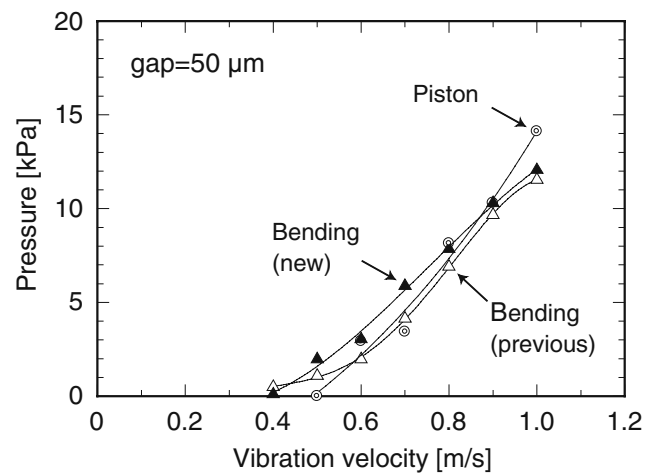**Fig. 10** Pump pressure vs. the gap size when the vibration velocity is 1.0 m/s

Fig. 12 Pump pressure vs. the vibration velocity when the gap size is fixed at 50 μm

4 Pump performance of the miniature pump using the newly designed disk transducer

4.1 Pump pressure characteristics

First, we investigated the pump pressure using the newly designed disk transducer. Driving frequency was 20.0 kHz. The vibration velocity at the disk center was fixed at 0.8 m/s. Figure 9 shows the pump pressure as functions of the gap size. In the figure, the pump pressure using a piston-vibrating surface is shown for a reference. The pump pressure became large as the gap size became small. The maximum pump pressure of 15.7 kPa was achieved when the gap size was 10 μm. Next, for vibration velocity of 1.0 m/s, we conducted the same experiments. The results are summarized in Fig. 10. The maximum pump pressure of 20.6 kPa was achieved when the gap size was 10 μm. In

both cases shown in Figs. 9 and 10, the new design gave the improved results compared with the previous design when the gap size was smaller than around 50 μm. However, the new design showed the similar values as the previous one when the gap size was larger than around 50 μm. The new design required the input power of 2.5 W for the pump pressure of 15 kPa although only 0.7 W with the previous design.

Next, we investigated the effects of the vibration velocity on the pressure. Figures 11 and 12 illustrate the pump pressure as functions of the vibration velocity at the disk center. The new design gave the improved results compared with the previous design when the gap size was 10 μm. On the other hand, there was little difference in the pump pressure for the previous and new design when the gap size was 50 μm.
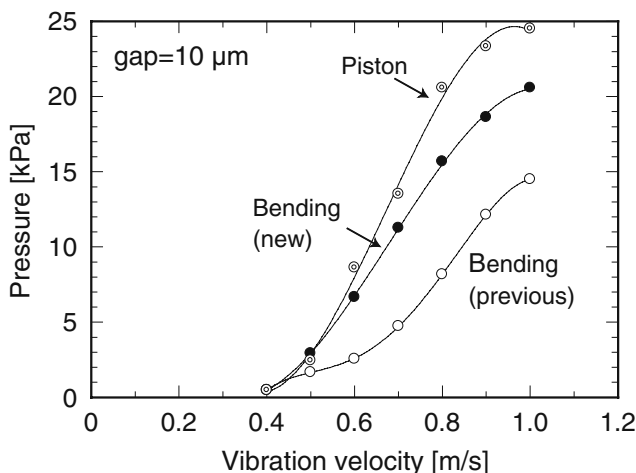

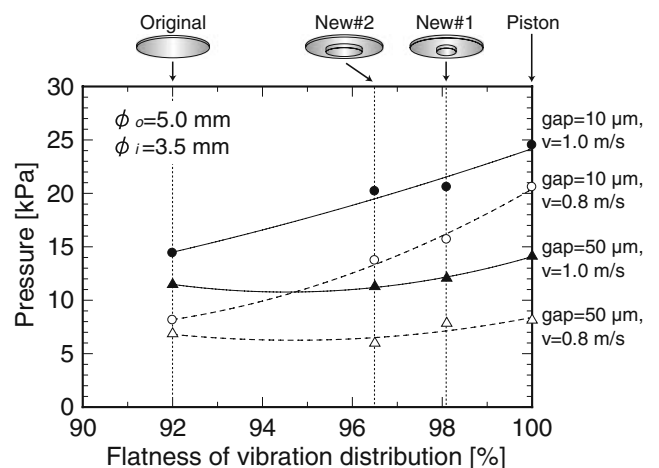**Fig. 11** Pump pressure vs. the vibration velocity when the gap size is fixed at 10 μm

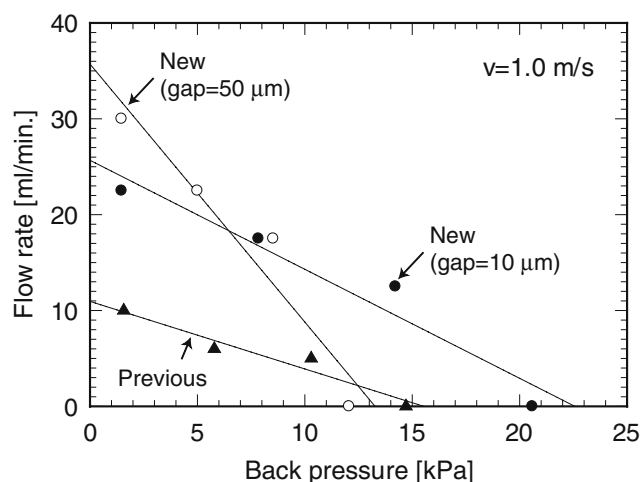**Fig. 13** Pump pressure vs. the flatness of the vibration distribution

Fig. 14 Flow rate vs. back pressure

4.2 Effects of the flatness of the vibration distribution

To make clear the relationships between the pump pressure and the flatness of the vibration distribution, the pressure is plotted as functions of the flatness in Fig. 13. In the figure, the results for the configuration of 96.5% in flatness are also shown for a reference. The pump pressure became large as the flatness became large when the gap size was small enough. On the other hand, the flatness has little effect on the pump pressure when the gap size was large.

4.3 Flow rate characteristics

Here, we investigate the flow rate characteristics. The vibration velocity at the disk center was maintained at 1.0 m/s. The gap size was fixed at 10 and 50 μm. Figure 14 shows the flow rate as functions of the back pressure. The flow rate became large as the back pressure became small. The maximum flow rate of 22.5 ml/min. was achieved when the gap size was 10 μm and the back pressure was

1.6 kPa. The flow rate became large as the gap size became large. The maximum flow rate of 30 ml/min. was achieved using the new design when the gap size was 50 μm.

5 Pump performance

The pump performance is summarized in Table 1. Here, water house power is defined as the maximum pump pressure times the maximum flow rate. Pump efficiency is defined as water house power divided by input power. The maximum pump pressure using the new design was improved about 1.4 times compared with the previous design, and approached the target value. The maximum flow rate using the new design was improved about 2.3 times compared with the previous design, and about only one-quarter of the target value.

6 Conclusions

In this paper, we introduced a miniature configuration for ultrasonic pump. The pump consists of a bending disk transducer with a small gap. To improve the pump performance, we optimize the configuration of the bending disk transducer. When the shape of the vibration distribution near the disk center became thick, the flatness of the vibration distribution improved 6% compared with the previous design.

Next, using new design disk, we achieved the maximum pump pressure of 20.6 kPa and the maximum flow rate of 22.5 ml/min. when the gap size was 10 μm and the vibration velocity at the disk center was 1.0 m/s. When the gap size was small enough, the pump pressure became large as the flatness became large. On the other hand, the flatness has little effect on the pump pressure when the gap size was large.

Table 1 Pump performance.

	Flatness	Max. pressure	Max. flow rate	Water house power	Input power	Pump efficiency
Piston-vibrating surface	100%	20.6 kPa	52 ml/min.	17.85 mW	52.7 W	0.034%
Original design	92.0%	14.8 kPa	10 ml/min.	2.47 mW	0.7 W	0.353%
New design	98.1%	20.6 kPa	22.5 ml/min.	7.73 mW	3.8 W	0.203%
Target value		20 kPa	100 ml/min.			

References

1. L. Jiang, J. Mikkelsen, J.-M. Koo, D. Huber, S. Yao, L. Zhang, P. Zhou, J.G. Maveety, R. Prasher, J.G. Santiago, T.W. Kenny, K.E. Goodson, IEEE Trans. Compon. Packag. Technol. **25**, 347 (2002)
2. S. Takahashi, H. Kitagawa, Y. Tomikawa, Jpn. J. Appl. Phys. **41**, 3442 (2002)
3. S. Takahashi, Y. Tomikawa, Jpn. J. Appl. Phys. **42**, 3098 (2003)
4. S. Takahashi, Y. Tomikawa, Jpn. J. Appl. Phys. **42**, 6135 (2003)
5. R. Luharuka, C.-F. Wu, P.J. Hesketh, Sens. Actuat. **112**, 187 (2004)
6. X. Yang, Z. Zhou, H. Cho, X. Luo, Sens. Actuat. **130–131**, 531 (2006)
7. G.-S. Park, K. Seo, IEEE Trans Magn **40**, 916 (2004)
8. Y. Okada, N. Yamashiro, K. Ohmori, T. Masuzawa, T. Yamane, Y. Konishi, S. Ueno, IEEE/ASME Trans. Mechatron. **10**, 658 (2005)
9. M. Hu, H. Du, S. Ling, IEEE/ASME Trans. Mechatron. **7**, 519 (2002)
10. A. Oki, M. Takai, H. Ogawa, Y. Takamura, T. Fukasawa, J. Kikuchi, Y. Ito, T. Ichiki, Y. Horiike, Jpn. J. Appl. Phys. **42**, 3722 (2003)
11. I. Ederer, P. Raetsch, W. Schullerus, C. Tille, U. Zech, Sens. Actuators **62**, 752 (1997)
12. N.-T. Nguyen, T.-Q. Truong, Sens. Actuat. **97**, 137 (2004)
13. R. Zengerle, J. Ulrich, S. Kluge, M. Richter, A. Richter, Sens. Actuat. **50**, 81 (1995)
14. O. Francais, I. Dufour, Sens. Actuat. **70**, 56 (1998)
15. P. Voigt, G. Schrag, G. Wachutka, Sens. Actuat. **66**, 9 (1998)
16. M. Takeuchi, K. Yamanouchi, Jpn. J. Appl. Phys. **33**, 3045 (1994)
17. G.-Q. Zhang, K. Hashimoto, M. Yamaguchi, Jpn. J. Appl. Phys. **35**, 3248 (1996)
18. A. Sano, Y. Matsui, S. Shiokawa, Jpn. J. Appl. Phys. **37**, 2979 (1998)
19. N.-T. Nguyen, R.M. White, IEEE Trans. Ultrason. Ferroelectr. Freq. Control **47**, 1463 (2000)
20. K. Chono, N. Shimizu, Y. Matsui, J. Kondoh, S. Shiokawa, Jpn. J. Appl. Phys. **43**, 2987 (2004)
21. C.-H. Yun, T. Hasegawa, K. Nakamura, S. Ueha, Jpn. J. Appl. Phys. **43**, 2864 (2004)
22. T. Hasegawa, J. Friend, K. Nakamura, S. Ueha, Jpn. J. Appl. Phys. **44**, 4658 (2005)
23. T. Hasegawa, K. Nakamura, S. Ueha, Ultrasonics **44**, 575 (2006)